



RESEARCH ARTICLE

The synoptic features of the autumn dust classes in Northern Saudi Arabia

Abdul-Wahab Mashat* and Adel Awad

Department of Meteorology, King Abdul Aziz University Jeddah, Saudi Arabia

Manuscript Info

Manuscript History:

Received: 12 December 2014
Final Accepted: 29 January 2015
Published Online: February 2015

Key words:

TOMS aerosol index, autumn dust, synoptic features, North Saudi Arabia

*Corresponding Author

Abdul-Wahab Mashat

Abstract

Three classes of autumn dust (narrow, moderate and widespread) have been identified over northern Saudi Arabia and were classified according to the values and spread of the Aerosol Index (AI) obtained from the TOMS satellite. Furthermore, the synoptic features that distinguish these classes were studied using NCAR/NCEP reanalysis data. Additionally, the frequency of the dust types observed on the surface accompanying these classes have been studied, and it has been demonstrated that Blowing Dust is the most frequent type, while the dust/sand storms occur with lesser frequency throughout autumn.

This synoptic study of the various classes of dust demonstrated the importance of the Azores and Siberian highs and the Indian low regarding the autumn dust over the northern Arabian Peninsula and also showed that the relative inter-position and the strength of these cyclonic and anticyclonic systems play an important role in the occurrence and intensity of the various classes of dust.

Moreover, the study showed that the intensity of the vertical motion, the decrease of the static stability over the Arabian Peninsula and its increase over the Mediterranean and Arabian Seas, in addition to the northern shift of the atmospheric systems at 500 hPa, are the main factors affecting the strength of the dust cases.

Copy Right, IJAR, 2015., All rights reserved

INTRODUCTION

The Arabian Peninsula and the surrounding deserts are considered as major dust-source regions in the world (Middleton, 1986; Prospero et al., 2002), and in addition to its local effects, the dust emitted from these areas is transported a great distance to East Asia (Tanaka et al. 2005; Al-Dabbas et al. 2010), as well as over the northern Arabian Sea (Kaskaoutis et al. 2010; Satheesh et al. 2010). Additionally, recent studies (Prasad et al. 2009; Gautam et al. 2010) have indicated that the dust emitted from this region plays an important role in mid-troposphere warming and therefore the melting of the Himalayan glaciers.

Dust emission requires suitable atmospheric conditions to release (Wang 2005). To identify these conditions, numerous studies have investigated the synoptic patterns (types) that accompany dust events. For example, Gaetani et al. (2012) specified the synoptic characteristics of the dust transported to the Mediterranean using a circulation-type method, while Hamidi et al. (2013) directly classified the synoptic characteristics of 12 severe dust storms that affected the Middle East and Southwest Asia using the NCEP-NCAR reanalysis data.

In addition, Awad and Mashat (2014) identified that the strong pressure gradient between the Azores high-pressure system and thermal low-pressure system over the Arabian Peninsula is the main factor that produced suitable conditions for the transport of a huge amount of dust from the Northeast African desert into Asia. Additionally, Awad 2014 studied the synoptic characteristics of the summer dust on the northern Arabian Peninsula and showed the importance of the relative positions of the Azores high and Indian low pressure systems in producing the dust cases. Furthermore, Awad and Mashat 2015 studied the synoptic features of the spring dust cases

over northern Saudi Arabia and demonstrated that the dust cases intensified when the pressure within the Azores high ridge over the Mediterranean and the Indian low decreased, and the trough that affected the northern Arabian Peninsula was extended northward.

By considering the unique conditions in the different regions and seasons regarding the synoptic features that affect dust cases, this study attempted to specify the main synoptic features of the classes of autumn dust in northern Saudi Arabia. In this study, dust cases were classified based on a threshold value of the aerosol index (AI) data collected by the TOMS satellite over the northern Arabian Peninsula, and the synoptic characteristics were studied using meteorological parameters from the National Centers for Environmental Prediction and the National Center for Atmospheric Research (NCEP/NCAR) reanalysis dataset.

The paper is organized as follows. In section 2, the data and methodology are described. Section 3 examines the results and synoptic characteristics of the composition of the various dust classes. The final section contains a discussion and the study conclusions.

2. Data and Methodology

The absorbing aerosols over land and water have been monitored for a long time by the Total Ozone Mapping Spectrometer (TOMS) Satellites (Torres et al., 1998), producing measurements known as the TOMS Aerosol Index (AI). The TOMS AI is composed of measurements of UV radiation at three discrete wavelengths (340, 360, and 380 nm), and its value is proportional to the optical depth and altitude of the dust, but the dust close to the surface produces a relatively weak response in the TOMS AI (Mahowald et al., 2003). A threshold for the AI value has been used as a condition for designating dust cases (Awad et al. 2014, Awad and Mashat 2015) and to mitigate the deficiency in the TOMS AI measurements (Hsu et al. 1999; Crosbie et al. 2014).

The global daily AI data have been collected from four different TOMS satellite instruments for 26 years, beginning in November 1978 and continuing until 2006, with a data gap from May 1993 to July 1996 and as spatial resolution of $1^\circ \times 1.25^\circ$ latitude/longitude.

The NCEP/NCAR Reanalysis Project collects six hours of meteorological data (Kalnay et al., 1996; Kistler et al., 2001), with a spatial resolution of $2.5^\circ \times 2.5^\circ$ latitude/longitude. The study domain is defined by the longitude 00°W - 70°E and latitude 10°N - 50°N .

The meteorological parameters used in this study are sea-level pressure (SLP), vertical motion at 500 hPa, wind components at 850 hPa, 500 hPa and 250 hPa, and geopotential height at 850 hPa and 500 hPa for the selected cases during the autumn months (September, October, and November) for the period from 1978 to 2006.

The dust cases were designated based on a value of the TOMS AI exceeding 1.216 (referred to as the threshold value). To determine the threshold value, first, the average and standard deviation of the AI were calculated for all cases that had at least one grid point with an AI greater than zero within the "checking zone", delineated by 26°N to 32°N and 35°E to 48°E (Figure 1). Then, the threshold value was calculated by the sum of half of the standard deviation and the average AI. The threshold calculated in this study is less than the values determined for spring (Awad and Mashat 2015) and summer (Awad 2014). The selected dust cases must have at least one grid point within a checking zone that achieved the threshold.

Applying the threshold to the AI data within the checking zone for all autumns in the study period revealed that the region has been affected by dust for 74.6% of the study period (Table 1). These selected cases have been classified into three classes according to the number of grid points that achieved the AI threshold as per the following conditions (73 total grid points in the checking zone were considered):

- (1) Narrow spread class (NS; the number of points within the checking zone that achieved a threshold value was less than or equal to 25, i.e., approximately 33% of the grid points);
- (2) Moderate spread class (MS; the number of points within the checking zone that achieved a threshold value was greater than 25 but less than or equal to 50, i.e., approximately 67% of the grid points); and
- (3) Wide spread class (WS; the number of points within the checking zone that achieved a threshold value was greater than 50, i.e., approximately 67% of the grid points).

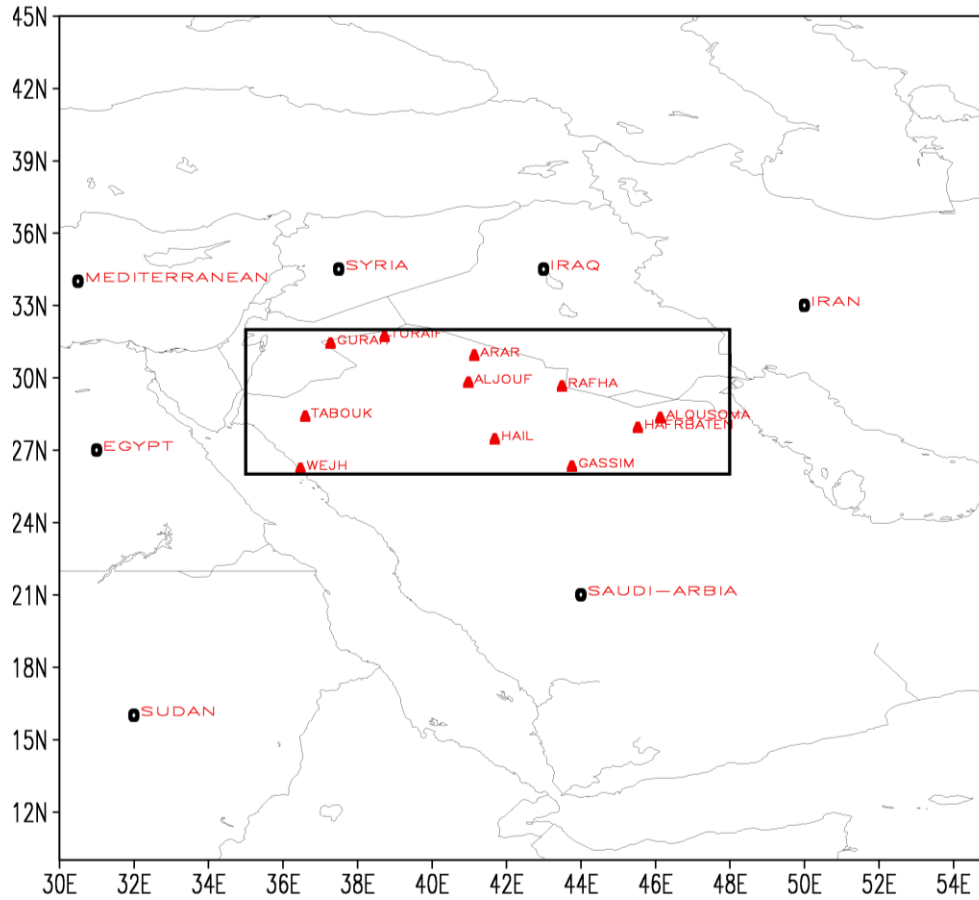


Figure 1. A map representing the relative location of the checking zone (black rectangle) with respect to nearby countries (represented by black circles). The surface stations inside the checking zone are represented by red triangles.

3. Results

The results describe briefly the statistics and detail the synoptic features of the autumn dust cases.

3.1 Statistical description

Applying the threshold value on the TOMS AI within the checking zone gives 1766 dust cases, which represents 74.6% of the autumn period. Furthermore, regarding the yearly distribution of these cases, figure 2 shows that most of the autumn dust cases are near the average, but some years were above average, e.g., 1996 and 2001, and some years were below average, e.g., 2004 and 2005. It is noteworthy that the TOMS satellites observed only one month (November) in 1978 and three days in 1980, which is the reason that these two years show only a few dust cases.

The classes of the selected cases, table 1, show that most of the dust cases are NS (62.1%), while the fewest are WS (9.5%). Furthermore, figure 2 shows that the NS cases were generally more numerous throughout the period except in 1984, during which MS cases were more numerous. Additionally, WS cases were more numerous than MS cases in 2003, and these cases were equal in 2002.

CLASS	ALL	NARROW	MODERATE	WIDE
NUMBER (RATIO)	1766 (74.6%) ₂	1097 (62.1%) ₁	502 (28.4%) ₁	167 (9.5%) ₁

Table 1. The number (percentage) of the dust cases belong to autumn classes and the total number of designated dust cases.

A bracket with the subscript 1 indicates the ratio with respect to the total wide spread events (1766 events), while the subscript 2 indicates the ratio with respect to the total autumn days (2366 days).

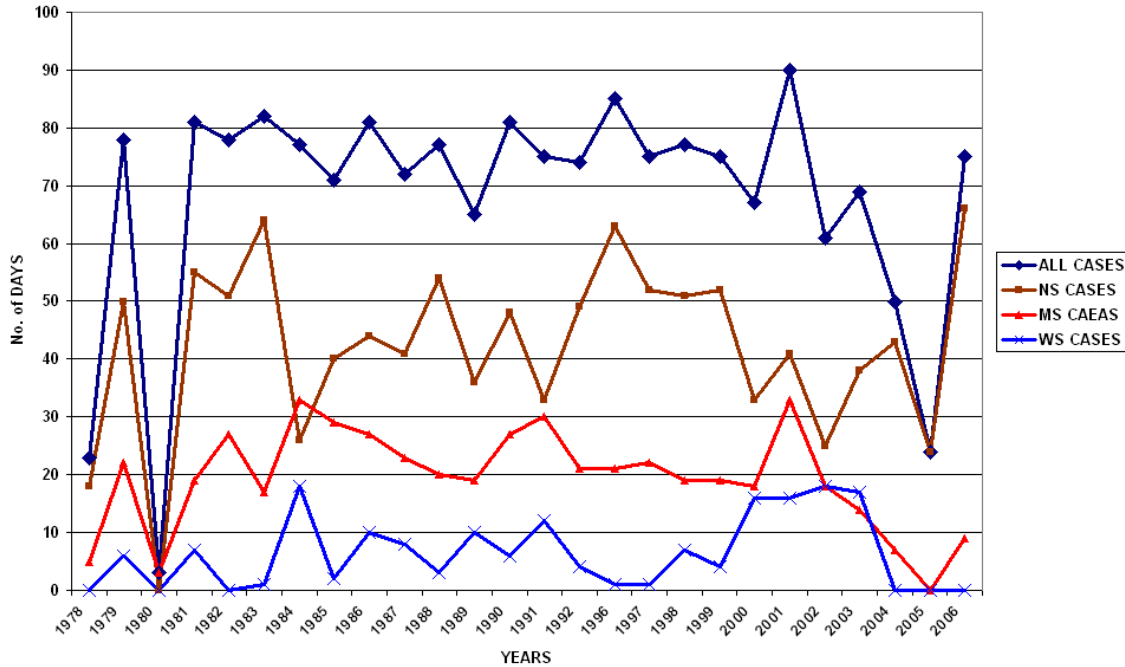


Figure 2. Yearly statistics for all selected dust cases and for the classes (Narrow (NS), Moderate (MS), and Wide (WS) spread) during the autumn from 1978 to 2006.

The distribution of the surface observations, table 2, demonstrated that the blowing dust (BD) is the most frequent dust type observed at the surface stations for the selected cases, followed by dust in suspension (DS) and then haze (HZ). The sand/dust storm types are least frequent, with approximately 6 observations each season.

Although the same distributions of the surface observations are repeated for various classes, DS is more frequently associated with the MS class than with the other classes. Additionally, the average numbers of the surface observations generally indicated that approximately two stations (1.7) observe one of the dust/sand types each day on the selected days, and this average decreases to 1.3 for the NS class and increases to 2.35 and 2.29 for the MS and WS classes, respectively.

CLS/DST	HZ	DS	BD	DST	SDST	AVERAGE
ALL	659	914	1267	108	46	1.701019
NS	355	382	608	63	25	1.314494
MS	222	402	499	39	16	2.348606
WS	82	130	160	6	5	2.293413

Table 2. The number of observations for individual dust/sand types (as described below) for all the selected dust cases (ALL) and classes NS, MS and WS.

Dust/sand types (HZ: haze, ww=5; DS: dust in suspension, ww=6; BD: blowing dust, ww=7; DST: dust storm ww=30-32; and SDST: severe dust storm, ww=33-35) at the stations within the checking zone for 26 autumn seasons.

3.2 Synoptic structures

This section describes the synoptic features of the various dust classes compared with the non-dust cases and between themselves at Mean Sea level pressure and the upper pressure levels 850, 500 and 250 hPa, in addition to the horizontal distribution of the dust.

3.2.1 Horizontal Dust Distribution

The horizontal distribution of the dust for non-dust cases, figure 3-a, shows that there is no appreciable amount of dust on the non-dust cases, but in contrast, a small amount of dust is found for NS, figure 3-b. For MS cases, figure 3-c, a considerable amount of dust began to appear, which was concentrated over the eastern and southern

regions of the checking zone. For WS, figure 3-d, the dust amount increased to cover the entire checking zone and extended northward to Turkey.

Generally, the horizontal distributions of the dust for the various classes show that the eastern Arabian Peninsula and Oman regions are highly affected regions for dust and have been classified as permanent dust areas, Mashat and Awad 2010.

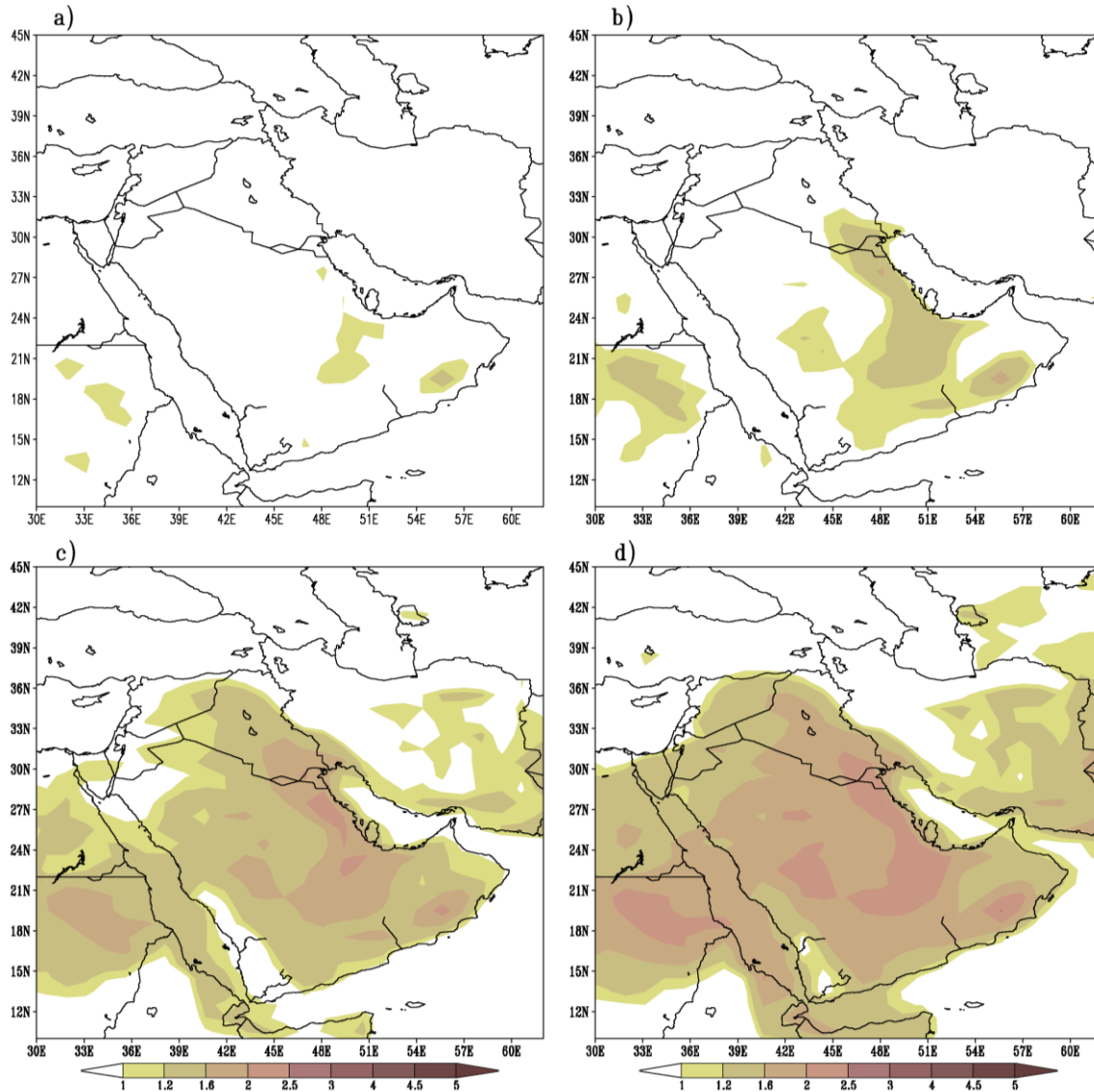


Figure 3. The horizontal distribution of the TOMS AI value (shaded) for the classes of the cases (a) non-dust, (b) narrow, (c) moderate and (d) wide spread.

3.2.2 Synoptic Features at Mean sea level Pressure

The general synoptic features on the surface for the non-dust cases, figure 4-a, are the Azores high pressure in the northwestern region at 1018 hPa and the Siberian high over the northeastern region at 1023 hPa. In addition, the Sudan low pressure at 1007 hPa, Sabziparvar et al., 2010, influenced the Arabian Peninsula through a trough extending over the eastern Red Sea and a weak trough extending from the Indian low over the western Arabian Gulf.

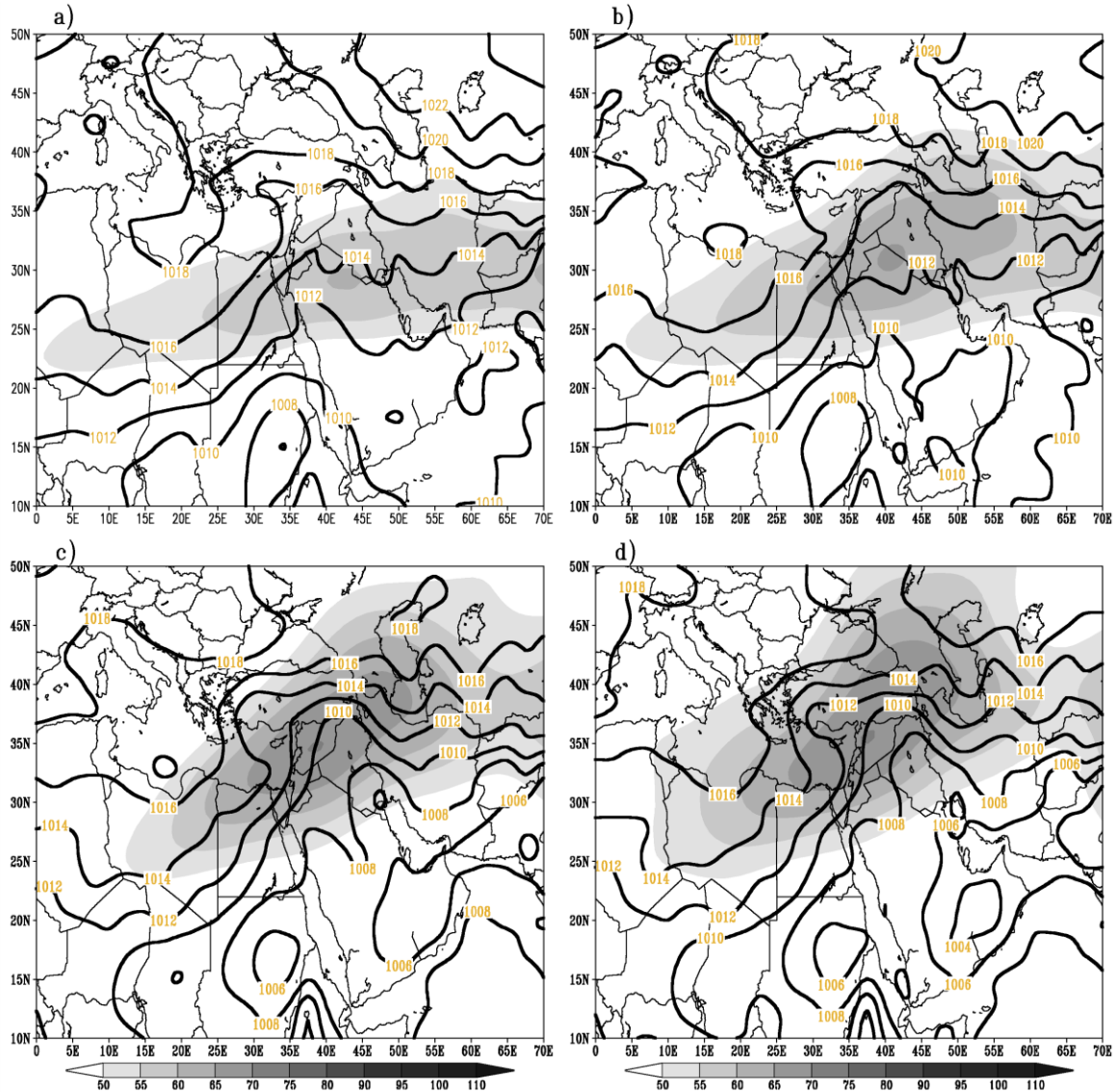


Figure 4. The distribution of the mean sea level pressure (SLP) (contours) and maximum wind speeds at 250 hPa (shaded) for various classes of cases (a) non-dust, (b) narrow, (c) moderate and (d) wide spread.

For the narrow spread class, figure 4-b, a high pressure cell at 1018 hPa appeared over the Libyan shore, which was separate from the northern high pressure belt that consists of the Azores and Siberian highs. Additionally, there was a low pressure cell at 1009 hPa, over the southern Arabian Peninsula, merging with the Sudan low and forming a wide trough over the western and a weak trough over the eastern Arabian Peninsula.

The Siberian high for the Moderate spread class, figure 4-c, was weakened (1017 hPa), while a high pressure cell over the Libyan shore was still at 1018 hPa. In addition, a low pressure cell at 1005 hPa was found over the southern Arabian Peninsula and appeared as an extension of the Indian Low. The low pressure cell over the southern Arabian Peninsula formed a low pressure belt with the Sudan low pressure (1006 hPa) and a low pressure cell (1007 hPa) over the southwestern Arabian Peninsula. The previous pressure systems integrated together and formed two troughs over the western and eastern Arabian Peninsula and a ridge over its center, but it is noteworthy that the eastern trough extended northward to Turkey.

Both the Siberian high (1017 hPa) and the high pressure cell over the Libyan shore (1017 hPa) were still weak for the Wide spread class, figure 4-d, but both of the low pressure cells over the southern Arabian Peninsula (1004 hPa) and the Sudan low (1006 hPa) were deepened. Additionally, for this class, the eastern Arabian Peninsula trough deepened and sharpened while the western trough flattened.

Moreover, the maximum wind at 250 hPa, figure 4, shows that the wind speed increased and the direction changed from west-east for the non-dust cases, figure 4-a, to southwest-northeast for the wide spread class, figure 4-d.

3.2.3 Synoptic Features and the vertical motion at 850 hPa

Two main synoptic systems at the pressure level of 850 hPa influenced the study region during the non-dust cases, figure 5-a, the cyclonic system over the northern region (1460 gpm) and the anticyclonic system over the southern region (1550 gpm), in addition to a weak cyclonic system over the central eastern area (1510 gpm) and an anticyclonic cell (1530 gpm) over the eastern Arabian Peninsula.

For the narrow spread class, figure 5-b, the northern cyclone weakened (1470 gpm) and shrank northward, and the southern anticyclone separated into two parts but still had a small anticyclonic cell over the eastern Arabian Peninsula.

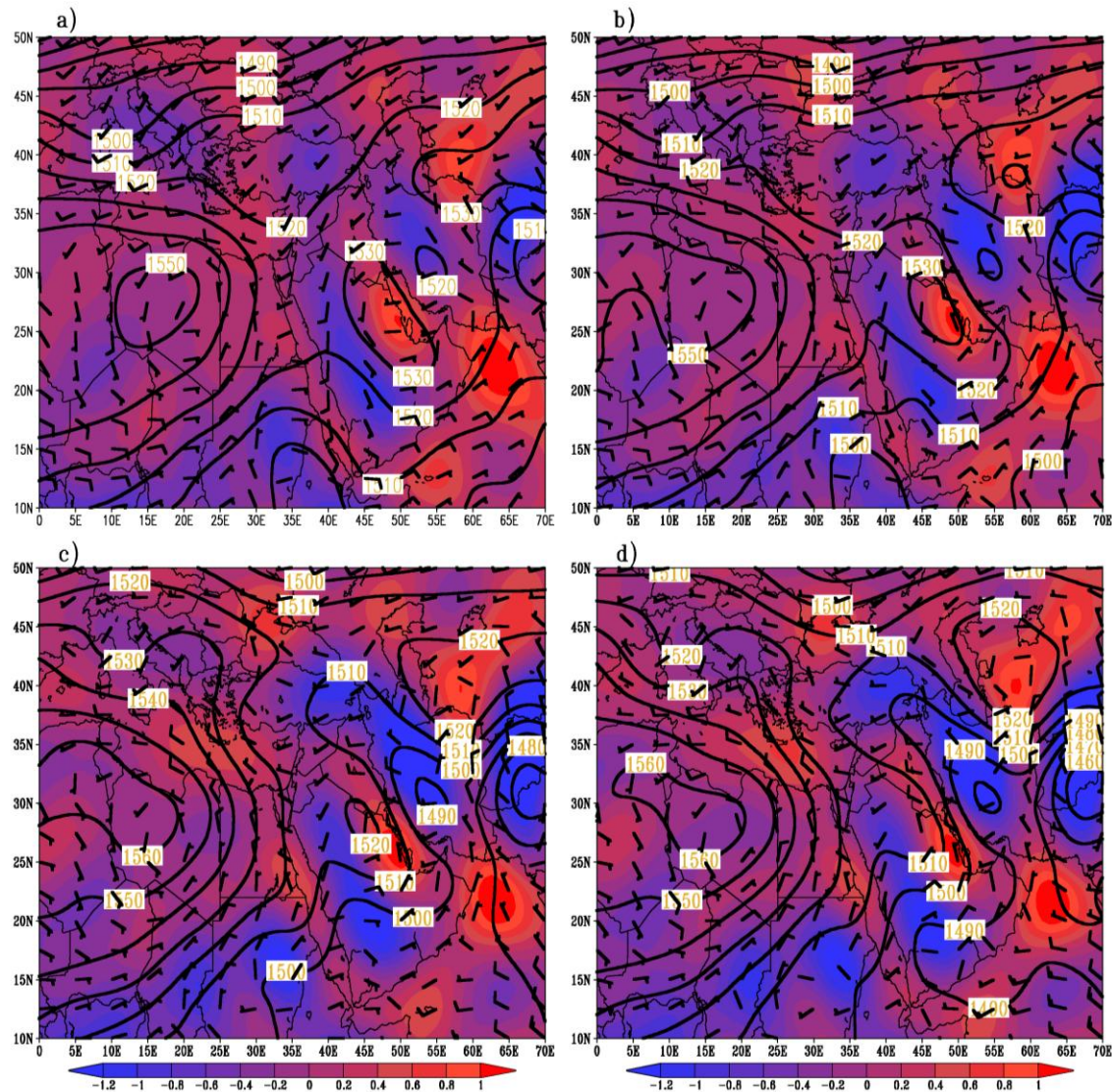


Figure 5. The geopotential height distribution (contours), wind vectors (barbs) and vertical motion (shaded) at the 850 hPa pressure level for different case classes (a) non-dust, (b) narrow, (c) moderate and (d) wide spread.

For the moderate spread class, figure 5-c, the anticyclone was pronounced in the western region, while the cyclonic system influenced the eastern region. Although the small anticyclonic cell appeared on the Arabian Peninsula (1520 gpm), a deep cyclone (1470 gpm) appeared over the eastern region and formed a trough over the Arabian Gulf.

The synoptic features for the wide spread class, figure 5-d, are similar to those for the moderate class, figure 5-c, but the anticyclonic cell over the Arabian Peninsula disappeared, the eastern cyclone became deeper (1460 gpm) and the trough over the Arabian Gulf deepened and sharpened. Furthermore, the distribution of the wind vectors over the Arabian Peninsula formed a pronounced anticyclonic cell during the strong dust cases.

In addition, the vertical motion at this pressure level (figure 5) shows a sequence of rising and subsiding motion cells over the Arabian Peninsula and the adjacent area, starting with a rising motion in east Africa, in addition to a subsiding cell over the Mediterranean. For the non-dust and narrow spread cases, the intensity of vertical motion cells weakened (Figures 5-a and 5-b, respectively) compared with the moderate and wide spread classes (Figures 5-c and 5-d, respectively).

3.2.4 Synoptic Features at 500 hPa and the static stability between 1000 and 500 hPa.

Generally, the atmospheric systems at the 500 hPa pressure level are the cyclonic over the northern and anticyclonic over the southern regions. However, during the non-dust and narrow spread cases (figure 6-a and 6-b, respectively), the main cyclonic center was deepened, with a minimum height of 5600 gpm, compared with 5660 gpm for the moderate and wide spread classes (Figure 6-c and 5-d, respectively). Additionally, the trough was oriented north to south and influenced the eastern Mediterranean during the non-dust and narrow spread cases, while it tended to the east during the strong cases. Moreover, the pressure of the anticyclonic system increased as the characteristics of the classes increased; for example, it was 5860 gpm for non-dust cases and 5880 gpm for wide spread cases. Furthermore, the relationship between the wind vectors and contours of the geopotential height indicated that the ageostrophic wind (baroclinicity) was higher during strong cases.

In contrast, the horizontal distribution of the static stability within the layer between 1000 and 500 hPa, figure 6, shows that a layer with less static stability over the Arabian Peninsula and Sahara was surrounded by stable layers over the Mediterranean and northern region and over the Arabian Sea. In addition, the stability over the Arabian Peninsula was lowest during the wide spread cases, figure 6-d, and highest during non-dust and narrow spread cases, figures 6-a and 6-b, respectively. Additionally, the stability over the Arabian and Mediterranean seas was highest during moderate and wide spreads cases, figures 6-c and 6-d, respectively, while it was lower for non-dust and narrow spread cases, figures 6-a, and 6-b, respectively.

4. Discussion and Conclusions

The statistical and synoptic features associated with the autumn dust cases over northern Saudi Arabia were examined using a threshold value (1.216 AI) for the Aerosol index from the TOMS satellites. The dust cases were selected and classified based on the TOMS AI distribution and values within the checking zone (delineated by 26°N to 32°N and 35°E to 48°E), which had achieved the threshold value.

The results of the selected dust cases during autumn demonstrated that more than two thirds of the time dust is present and that most of these cases are NS cases (62.1%), while the fewest are WS cases (9.5%).

Furthermore, the distribution of the observed surface dust types demonstrated that the Blowing Dust type is the most frequent, while the sand/dust storm types are the least frequent. Generally, approximately two stations observe one of the dust/sand types each day on the designated dust days, while the average number of the stations decreases to 1.3 for the NS class and increases to 2.35 and 2.29 for the MS and WS classes, respectively.

Moreover, the horizontal distribution of the aerosols shows that the dust amount increases and extends northward as the characteristics of the class intensify and indicate that the eastern Arabian Peninsula and Oman regions are highly affected by dust.

In addition, the surface synoptic features show that two different pressure systems influence the region, the Indian low pressure on the southeastern Arabian Peninsula and the Sudan low pressure over southeastern Sudan and the Azores high system over the northwestern region and the Siberian high over the northeastern region. Furthermore, the high pressure systems weaken and the low pressure systems strengthen as the characteristics of the dust class intensify. These mechanisms allow a deep trough to form over the eastern Arabian Peninsula during relatively strong dust events. Additionally, the maximum wind speed at 250 hPa increases and its direction changes anticlockwise as the characteristics of the class intensify.

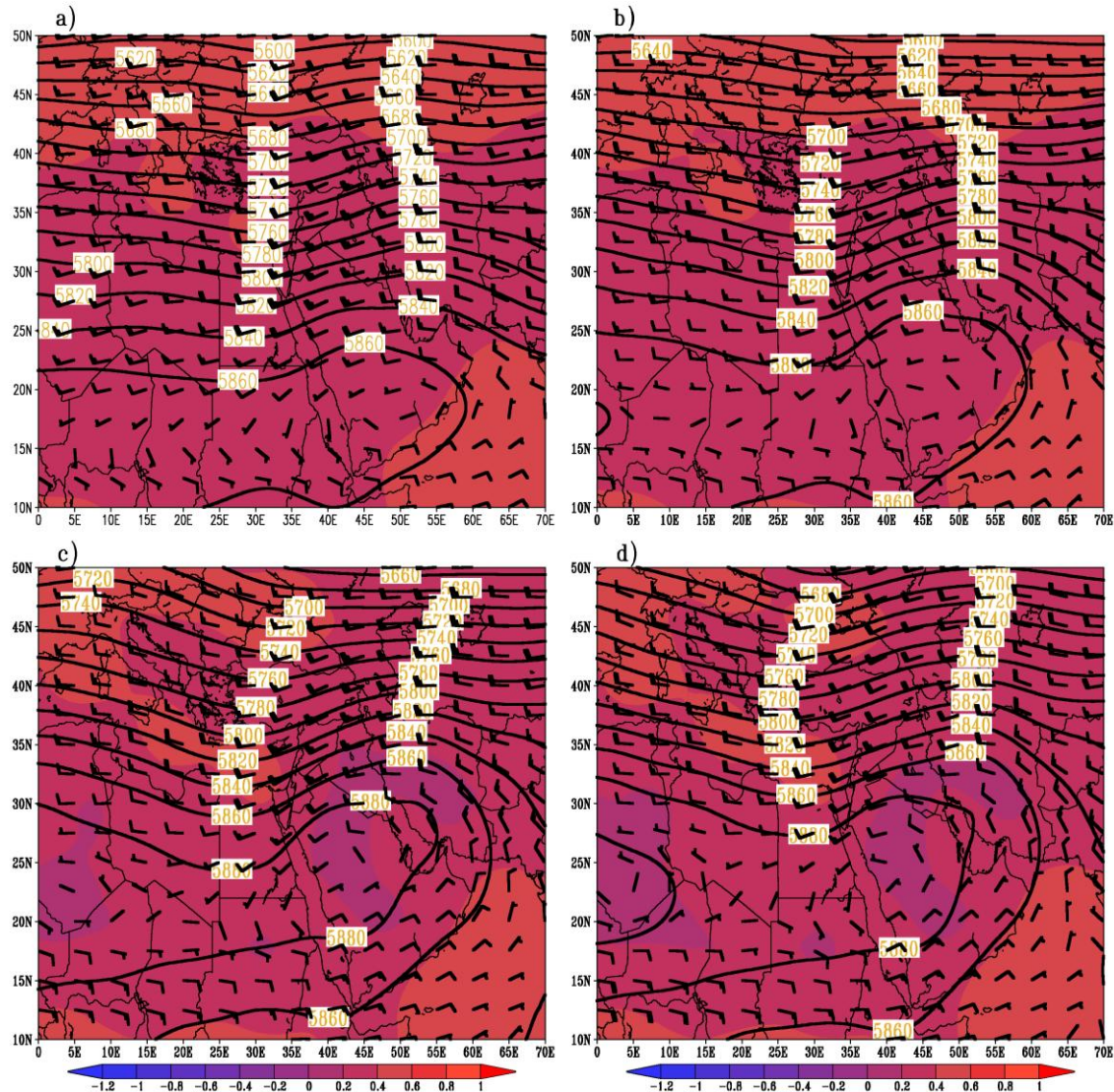


Figure 6. The geopotential height distribution (contours) and wind vectors at the 500 hPa pressure level (barbs) and the static stability between 1000 hPa and 500 hPa (shaded) for different classes of cases (a) non-dust, (b) narrow, (c) moderate and (d) wide spread.

In contrast, the synoptic features at the pressure level of 850 hPa indicate that the deepening of the eastern cyclone and the strength of the western anticyclone, in addition to the deep trough over the Arabian Gulf, increase as the characteristics of the class intensify. Furthermore, the cyclonic and anticyclonic systems are arranged north-south for the non-dust and the weak dust cases and change to west-east for the strong dust cases. In addition, the vertical motion at this pressure level demonstrates that the intensity of the vertical motion cells strengthens as the characteristics of the class increase.

The atmospheric systems at the 500 hPa pressure level show that the northern cyclone weakens while the southern anticyclonic gains strength as the characteristics of the classes increase, as if the atmospheric systems shift northward as the dust case intensifies.

Additionally, the horizontal distribution of the static stability shows that the stability over the Arabian Peninsula decreases while increasing over the Mediterranean and Arabian Seas as the characteristics of the dust cases intensify.

The previous discussion indicates that the atmospheric synoptic features associated with the autumn dust events are sufficient to distinguish between the various dust events, and the changes in the strength and inter-position of the synoptic systems are strongly related to the dust characteristics. Thus, we could say with high confidence that the

autumn dusts are synoptically triggered, or the main mechanisms of the autumn dust are synoptic factors rather than dynamic factors, as in summer, Awad 2014.

References

- Al-Dabbas MA, Abbas MA, Al-Khafaji RM (2010) Dust storms loads analysis—Iraq. Arab J Geosci 5(1):121–131
- Awad A. M. 2014: Characteristics of Atmospheric Systems Accompany with Summer Dust over Northern Arabian Peninsula. Int. J. of Adv. Res. 2 (12), 821-833. (ISSN 2320-5407) www.journalijar.com.
- Awad AM, Mashat AS (2014) Synoptic features associated with dust transition processes from North Africa to Asia. Arab J Geosci. 7(6): 2451-2467; doi:10.1007/s12517-013-0923-4.
- Awad AM, Mashat AS, Abo Salem FF (2014) Diagnostic study of spring dusty days over the southwest region of the Kingdom of Saudi Arabia. Arab J Geosci.doi:10.1007/s12517-014-1318-x.
- Awad AM, Mashat AS (2015) Synoptic characteristics of spring dust days over northern Saudi Arabia. Air QualAtmos Health. doi:10.1007/s11869-015-0320-0
- Crosbie, E.; Sorooshian, A.; Monfared, N.A.; Shingler, T.; Esmaili, O.A multi-year aerosol characterization for the greater Tehran Area using satellite, surface, and modeling data. Atmosphere 2014, 5, 178–197.
- Gaetani, M., Pasqui, M., 2012. Synoptic patterns associated with extreme dust events in the Mediterranean Basin. Regional Environmental Change, Springer-Verlag, 1e14.http://dx.doi.org/10.1007/s10113-012-0386-2.
- Gautam R, Liu Z, Singh RP, Hsu NC (2009) Two contrasting dust-dominant periods over India observed from MODIS and CALIPSO data. Geophys Res Lett, 36, L06813, doi:10.1029/2008GL036967.
- Hamidi, M., Mohammad, R. K., Yaping, S., 2013: Synoptic Analysis of Dust Storms in the Middle East.Asia-Pacific J. Atmos., Sci., 49(3), 279-286.
- Hsu NC, Herman JR, Torres O, HolbenBN, Tanre D, Eck TF, Smirnov A, Chatenet B, Lavenu F. Comparisons of the TOMS aerosol index with sun-photometer aerosol optical thickness: results and applications. J. Geophys. Res. 1999; 104:6269–6279.
- Kalnay E, Kanamitsu M, Kistler R, Collins W, Deaven D, Gandin L ,IridellM, Saha S, White G, WoollenJ,Zhu Y ,Chelliah M, Ebisuzaki W, Higgins W ,JanowiakJ,Mo KC, Ropolewski C, Wang J, Leetma A, Reynolds R, JenneR,Joseph D (1996) The NCEP/NCAR 40-year Reanalysis project. Bull Am MeteorolSoc 77: 437–471.
- Kaskaoutis DG, KalapureddyMCR, Krishna Moorthy K, Devara PCS, Nastos PT, Kosmopoulos PG, Kambezidis HD (2010) Heterogeneity in pre-monsoon aerosol types over the Arabian Sea deduced from shipboard measurements of spectral AODs. AtmosChemPhys 10, 4893-4908.
- Kistler R, Collins W, Saha S, White G, Woollen J, Kalnay E, Chelliah M, Ebisuzaki W, Kanamitsu M, Kousky V, vandenDool H, Jenne R, Fiorino M (2001) The NCEP/NCAR 50-year Reanalyses: Monthly CD-ROM and documentation. Bull Am MeteorolSoc 82: 247–267.
- Mahowald NM, Luo C, delCorralJ, Zender C (2003)Interannual variability in atmospheric mineral aerosols from a 22-year model simulation and observation data. J Geophys Res 108 (D12).doi: 10.1029/2002 JD002821.
- Mashat Abdul Wahab, Awad A. M.2010: The Classification of the Dusty areas over the Middle-East. Bull. Fac. Sci., Cairo Univ. 78(A): 1-19.
- Middleton NJ (1986) Dust storms in the Middle East. J. Arid Environ. 10, 83-96.

Prasad AK, Yang KHS, El-Askary HM, Kafatos M (2009) Melting of major glaciers in the western Himalayas: evidence of climatic changes from long term MSU derived tropospheric temperature trend (1979-2008). *Ann Geophys* 27, 4505-4519.

Prospero JM, Ginoux P, Torres O, Nicholson SE, Gill TE (2002) Environmental characterization of global sources of atmospheric soil dust identified with the Nimbus 7 total ozone mapping spectrometer absorbing aerosol product. *Reviews of Geophys.* 40, 2–31.

Sabziparvar, A. A., A. Parandeh, H. Lashkari, and H. Yazdanpanah (2010), Mid-level synoptic analysis of flood-generating systems in south-west of Iran (case study: Dalaki watershed river basin), *Nat. Hazards Earth Syst. Sci.*, 10(11), 2269–2279, doi:10.5194/nhess-10-2269-2010.

Satheesh SK, Vinoj V, MoorthyKK (2010) Assessment of aerosol radiative impact over oceanic regions adjacent to Indian subcontinent using Multisatellite analysis. *Adv in Meteorol* ID 139186, doi:10.1155/2010/139186.

Tanaka TY, Kurosaki Y, Chiba M, Matsumura T, Nagai T, Yamazaki A, Uchiyama A, Tsunematsu N, Kai K (2005) Possible transcontinental dust transport from North Africa and the Middle East to East Asia. *Atmos Environ* 39(21):3901–3909

Torres O, BhartiaPK, Herman JR, Ahmad Z, Gleason K (1998) Derivation of aerosol properties from satellite measurements of backscattered ultraviolet radiation: theoretical basis. *J Geophys Res* 103: 17099–17110.